analytical chemistry

ARTICLE

pubs.acs.org/ac

Micropatterned Aptasensors for Continuous Monitoring of Cytokine Release from Human Leukocytes

Ying Liu, Jun Yan, Michael C. Howland, Timothy Kwa, and Alexander Revzin*

Department of Biomedical Engineering, University of California, Davis, California 95616, United States

Supporting Information

ABSTRACT: We report the development of a microdevice for detecting local interferon gamma (IFN-γ) release from primary human leukocytes in real time. Our microdevice makes use of miniature aptamer-modified electrodes integrated with microfluidics to monitor cellular production of IFN-γ. The aptamer species consists of a DNA hairpin molecule with thiol groups on the 3′-end for self-assembly onto Au electrodes. A redox reporter is covalently attached at the 5′-end for electrochemical sensing. This aptasensor has excellent sensitivity for IFN-γ (<60 pM detection limit) and responds to the target analyte in real time without additional washing or labeling steps. Aptamer-functionalized electrode arrays are fabricated on glass slides containing poly(ethylene glycol) (PEG) hydrogel patterns designed to expose glass regions adjacent to electrodes while protecting the remainder of the surface from nonspecific adsorption. The micropatterned substrates are integrated with PDMS microfluidic channels and incubated with T-cell-specific antibodies (Ab) (anti-CD4). Upon injection of blood, leukocytes are bound to Ab-modified glass regions in proximity to aptasensors. Cytokine release from captured cells is triggered by mitogenic activation and detected at the aptamer-modified electrodes using square wave voltammetry (SWV). The IFN-γ signal is monitored in real time with signal appearing as early as 15 min poststimulation from as few as 90 T cells. The observed IFN-γ release profiles are used to calculate an initial IFN-γ production rate of 0.0079 pg cell^{-1} h^{-1} upon activation. The work described here represents an important step toward development of aptasensors for immune cell analysis and blood-based diagnostics.

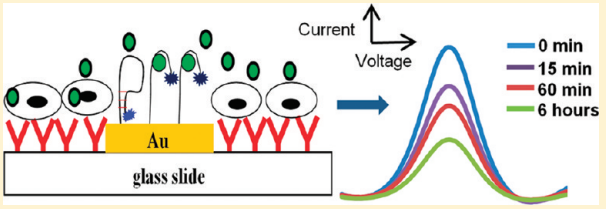

Leukocytes represent a heterogeneous population of immune cells that play a central role in mounting defenses against viral or bacterial infection.[1−3] Leukocytes orchestrate immune responses by releasing cytokines—small proteins capable of inducing a variety of cellular responses including proliferation and chemotaxis.[4,5] Given the heterogeneity of leukocytes and different roles played by different cell types in the immune response, it is desirable to analyze cytokine production in specific leukocyte subsets. IFN-γ is an important inflammatory cytokine used to evaluate cellular immune response to pathogens and infectious diseases. For example, production of interferon gamma (IFN-γ) by T cells correlates with the body's ability to mount a vigorous immune response[6] and is used to identify antigen-specific T cells in diseases such as human immunodeficiency virus (HIV) or tuberculosis.[7,8] It should be noted that cytokines such as IFN-γ may be produced by multiple leukocyte subsets (e.g., neutrophils, CD4 T cells, and CD8 T cells). Therefore, measurements of cytokine concentration in blood are insufficient to identify cytokine-secreting leukocyte subsets.

At the present time, two methods are used for detecting cytokine production in specific leukocyte subsets: (1) flow cytometry coupled with intracellular cytokine staining and (2) enzyme-linked immunospot (ELISpot) assay.[5,9−11] Both approaches are robust, functional, and well established in immunology laboratories. However, these approaches have shortcomings. Flow cytometry can detect intracellular cytokines but requires fixation of cells prior to analysis. This limits the suitability of flow cytometry for monitoring cytokine secretion in live cells. ELISpot may be used for detecting extracellular cytokines from live cells; however, this technology only detects the frequency of cytokine-producing cells in a given sample and does not connect cytokine release to specific cells. Both approaches are labor intensive and time consuming and do not provide information about the dynamics of cytokine release. We aim to resolve these limitations by developing a biosensor based around the spatially directed capture of cells and the monitoring of cytokine release using electrochemically functionalized aptamers.

Micropatterning and microfabrication can be used to organize cells into large arrays for high-throughput screening, to place cells near sensing elements, and to confine cells in small volumes for sensitive detection.[12,13] Several groups have been developing micropatterned surfaces for immune cell analysis.[14−21] Our laboratory has reported on the development of antibody (Ab) microarrays and Ab micropatterns for capturing leukocytes and detecting cell-secreted cytokines.[22−24] However, Ab-based immunoassays involve multiple staining/washing steps and offer limited information about dynamics of cytokine release from cells. It may be possible to detect cell-secreted proteins in real time, for example,

Received: August 11, 2011
Accepted: September 26, 2011

   dx.doi.org/10.1021/ac202117g | *Anal. Chem.* XXXX, XXX, 000–000

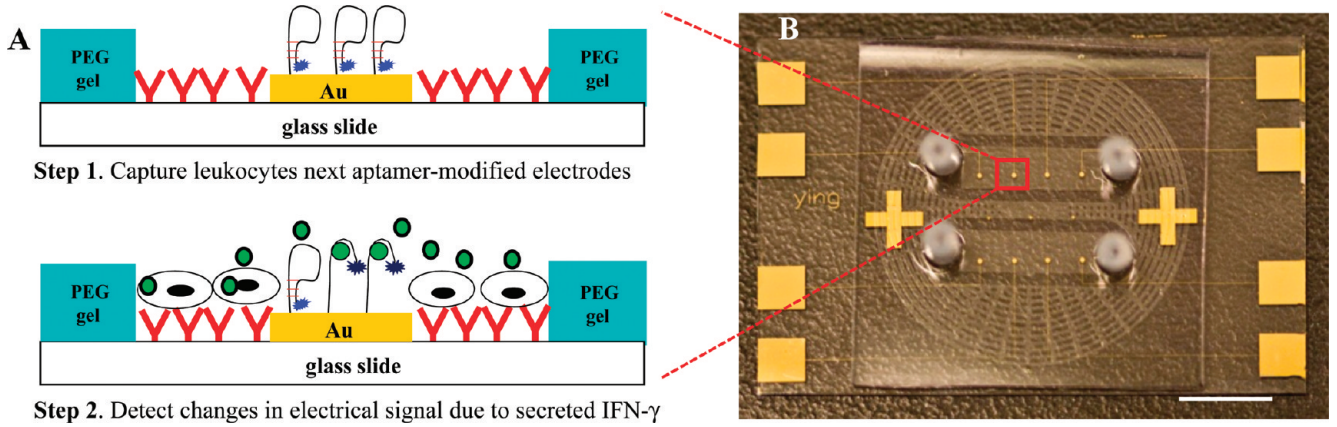

Figure 1. (A) Schematic of the sensing area layout. Au electrode arrays fabricated on glass slides are surrounded by PEG hydrogel and incubated with T-cell-specific antibodies. Upon injection of blood, leukocytes are bound on Ab-modified glass regions next to aptasensors. Cytokine release is detected at the aptamer-modified electrodes by an aptamer recognition layer consisting of DNA hairpin-containing redox reporters (B). These micropatterned substrates are integrated inside PDMS microfluidic channels (scale bar is 4 mm). There are 4 individually addressable aptasensing electrodes per channel.

using Ab-functionalized SPR devices.[25,26] However, the need to couple a cell capture device to an SPR instrument increases the complexity of the measurement and limits the possibility of monitoring molecules secreted by small groups of cells or single cells.

Aptamers offer a number of advantages over antibodies including improved chemical/thermal stability and reusability. Owing to their simple molecular structure, aptamers may be converted into fluorescent[27−29] or electrochemical[30−32] beacons that transduce analyte binding events directly, without the need for additional reagents or labeling steps. While there are reports of aptamer-based biosensors employed for clinical sample analysis in the literature[33−36] and our laboratory has recently described an aptamer-based electrochemical biosensor for detection of exogenous IFN-γ,[37] we are not aware of studies describing aptasensors deployed in the immediate vicinity of cells for direct monitoring of cell-secreted proteins such as cytokines.

In the present paper we describe a microdevice employing arrays of miniature aptasensor-functionalized electrodes for detection of IFN-γ release from leukocytes. The sensing mechanism is based on a change in hairpin conformation due to binding of cell-secreted cytokine molecules. This microdevice, pictured in Figure 1, consists of aptamer-modified electrode arrays integrated with microfluidics. Sensing electrodes are packaged in poly(ethylene glycol) (PEG) so as to define cell attachment sites in the proximity of each electrode. These attachment sites were modified with anti-CD4 Ab to promote CD4 T cells binding. Upon infusing RBC lysed blood into fluidic channels, leukocytes are captured next to sensing electrodes and stimulated to produce cytokines. IFN-γ released by cells is then detected at the neighboring sensing electrodes using square wave voltammetry (SWV) (see Figure 1A). Importantly, cytokine release by CD4 T cells can be monitored continuously and allows one to determine the rate of IFN-γ production. To the best of our knowledge, this is the first report describing aptasensor electrodes for monitoring local protein release from live cells in real time.

MATERIALS AND METHODS

Materials. Phosphate-buffered saline (PBS), 10×, without calcium and magnesium, paraformaldehyde (PFA), Na_4EDTA, $KHCO_3$, NH_4Cl, anhydrous toluene (99.9%), potassium ferricyanide, 11-mercaptoundecanoic acid (MUA), 200-proof ethanol, tris(hydroxymethyl) aminomethane buffer (Tris buffer), poly(ethylene glycol) diacrylate (PEG-DA, MW 575), and 2-hydroxy-2-methyl-propiophenone (photoinitiator) were purchased from Sigma-Aldrich. Chromium etchant (CR-4S) and gold etchant (Au-5) were purchased from Cyantek Corp. (Fremont, CA). Positive photoresist (AZ 5214-E IR) and developer solution (AZ300 MIF) were bought from Mays Chemical (Indianapolis, IN). 3-Acryloxypropyl trichlorosilane, was purchased from Gelest, Inc. (Morrisville, PA). Silane adhesion promoter, 3-acryloxypropyl trichlorosilane, was purchased from Gelest, Inc. (Morrisville, PA). Monoclonal purified mouse antihuman CD4 Abs (13B8.2) were obtained from Beckman-Coulter (Fullerton, CA). Antihuman CD3-FITC (UCHT1) and anti-CD4-PE (L120) were used for immunostaining of surface-bound cells and purchased from BD Pharmingen. Human recombinant IFN-γ was from R&D Systems (Minneapolis, MN). T cells activation reagents, phorbol 12-myristate 13-acetate (PMA) and ionomycin, were purchased from Sigma-Aldrich (St. Louis, MO). Cell culture medium RPMI 1640 with L-glutamine was purchased from VWR. Medium was supplemented with fetal bovine serum (FBS), and penicillin/streptomycin purchased from Invitrogen. Glass slides (25 mm × 75 mm × 1 mm) were obtained from VWR (West Chester, PA). 4-(2-Hydroxyethyl)-1-piperazineethanesulfonic acid (HEPES), sodium bicarbonate ($NaHCO_3$) (all reagent grade), 6-mercapto-1-hexanol (MCH), and tris(2-carboxyethyl)phosphine hydrochloride (TCEP) were purchased from Sigma-Aldrich (St. Louis, MO); methylene blue (MB), carboxylic acid, and succinimidyl ester were received from MB-NHS, Biosearch Technologies, Inc. (Novato, CA). All chemicals were used without further purification. The 34-mer IFN-γ-binding aptamer sequence (IDT Technologies, San Diego, CA) was as follows: 5′-NH_2-C_6-GGGGTTGGTTGTGTTGGGTGTTGTGTCCAACCCCC3-SH-3′. The aptamer was modified at the 3′-terminus with a C6-disulfide [$HO(CH_2)_6-S-S-(CH_2)_6-$] linker and at the 5′-end with an amine group for redox probe (MB) conjugation. The aptamer was dissolved in 1× PBS buffer (pH 7.4).

Fabrication of Electrode Arrays. The layout of an electrode array was designed in AutoCAD and converted into plastic

dx.doi.org/10.1021/ac202117g |*Anal. Chem.* XXXX, XXX, 000–000

transparencies by CAD Art Services (Portland, OR). To fabricate electrode arrays, glass slides (75 mm × 25 mm) were sputter coated with a 15 nm Cr adhesion layer and 100 nm Au layer (Lance Goddard Associates, Santa Clara, CA). The electrodes were fabricated using standard photolithography and metal-etching processes.[38] The photoresist layer was not removed immediately after metal etching but was employed to protect underlying Au regions during the silane modification protocol described below. The etching of Au/Cr layers created a pattern of eight 300 μm diameter electrodes individually connected to a 2 mm × 2 mm contact pad via leads that were 15 μm wide. Wires were soldered to contact pads to connect electrode arrays to a home-built multiplexing setup capable of automated data collection from electrode arrays during the electrochemistry experiments.

Formation of PEG Hydrogel around Electrodes. The glass substrates with photoresist-covered Au electrodes were modified with an acrylated silane coupling agent using a previously reported protocol.[39] Silanization was necessary to ensure covalent anchoring of hydrogel structures onto glass substrates. After silane modification, substrates were sonicated in acetone for 2 min to remove photoresist and then placed in an oven for 3 h at 100 °C to fully cross-link the silane layer. Integration of Au microelectrodes with nonfouling PEG hydrogel micropatterns was performed as follows. Prepolymer solution containing PEG-diacrylate (PEG-DA) (MW 575) and 2% (v/v) photoinitiator was spin coated at 800 rpm for 4 s onto glass slides containing Au electrode patterns. A photomask was placed on top of the liquid layer of PEG-DA precursor solution and aligned to fiduciary marks using an upright microscope or a mask aligner. Then the sample was exposed through a chrome/soda lime photomask to UV radiation for 1 s at 60 mJ/cm^2 using an OmniCure series 1000 light source using a Cannon PLA-501F mask aligner. The regions of PEG-DA exposed to UV light underwent radical polymerization and became cross-linked, while unexposed regions were dissolved in DI water after 5 min of development.

Ab Immobilization for T Cells Attachment. In order to ensure excellent sensitivity of the electrochemical aptasensors, the electrode regions must be protected from nonspecific deposition of Ab molecules during this process. For this purpose, we employ a protective sacrificial layer of alkanethiols. Micropatterned surfaces were modified with anti-CD-4 Ab. Au electrodes were modified with an alkanethiol layer by incubation with 1 mM MUA for 2 h to protect the electrode surface during Ab modification. Subsequently, micropatterned surfaces were incubated with anti-CD4 Ab (0.1 mg/mL in 1× PBS). As a result, Ab molecules deposited on both Au electrodes and neighboring silanized glass regions; however, the electrodes were regenerated or "cleaned" by reductive desorption of the MUA/Ab layer. This reductive desorption protocol has been described by us in detail previously.[38] Briefly, substrates were placed into a custom-made Plexiglas electrochemical cell using a three-electrode system. A potentiostat (CH Instruments 842B, Austin, TX) was used to apply a reductive potential (−1.2 V vs Ag/AgCl) for 60 s to individually addressable Au regions. In this approach, electrode arrays are incubated with an alkanethiol (MUA). This layer serves as a protective layer during the Ab deposition process. Incubation of the micropatterned surfaces in solution of anti-CD4 results in physical adsorption of Ab onto glass and electrode regions alike; however, electrodes are "cleaned" by applying reductive voltage and removing both the protective alkanethiol layer and the nonspecifically deposited Ab selectively from the electrode surfaces. Ferricyanide cyclic voltammetry (CV) was used to characterize electrode protection and deprotection steps. Cyclic voltammetry (CV) at a scan rate of 100 mV/s with ferricyanide serving as a redox reporter was used to characterize the electrode surface properties before and after disruption of the alkanethiol−Ab layer. These results (shown in Figure S1, Supporting Information) demonstrate that passivation with a sacrificial layer effectively protects the electrode surfaces during Ab immobilization, ensuring that electrodes are available for subsequent aptamer assembly. After this step, Au electrode arrays were ready for aptamer modification. Upon deprotection, the electrodes are incubated with a dual-functionalized hairpin aptamer containing MB moiety at one end and a thiol group at the other. The thiol group allows for coupling to the electrode surface via sulfur−gold bond formation, while methylene blue serves as a redox reporter. It is important to note that the surrounding hydrogel regions are unaffected by these processes and remain nonfouling after Ab and aptamer functionalization. Results demonstrating selective protein deposition on micropatterned sensing surfaces are presented in Figure S2, Supporting Information.

Aptamer Immobilization on Electrode Arrays. The MB-tagged thiolated aptamer was prepared using a procedure similar to that described previously.[37,40] Briefly, NHS-labeled MB was conjugated to the 3′-end of an amino-modified DNA aptamer through succinimide ester coupling. The conjugation efficiency was estimated by MALDI-MS analysis to be 30%. Aptamer molecules were immobilized on electrode arrays. Prior to modification of the electrodes, aptamer stock solution (0.02 mM) was reduced in 10 mM TCEP for 1 h to cleave disulfide bonds. This solution was then diluted in PBS buffer to achieve the desired aptamer concentration (0.5 μM, the optimal concentration for IFN-γ binding[37]). For aptamer immobilization, the Au electrodes were kept in an aqueous solution for 2 h in the dark. Following incubation, the electrodes were rinsed with copious amounts of DI water and then immersed in an aqueous solution of 3 mM 6-mercapto-1-hexanol solution (MCH) for 1 h to displace nonspecifically adsorbed aptamer molecules and to passivate the electrode surface.

Integration of Aptasensors with Microfluidics and Capture of Leukocytes. Microfluidic channels were fabricated out of poly(dimethyl siloxane) (PDMS) using standard soft lithography approaches.[41] These channels were secured on top of aptamer-modified electrodes using vacuum suction as described previously.[22,23,42] The microfluidic device contained two flow chambers with width × length × height dimensions of 3 × 10 × 0.1 mm and a network of independently addressed auxiliary channels used to provide vacuum. Figure 1B shows a typical microfluidic device integrated with an array of sensing electrodes.

IFN-γ detection experiments were performed using red blood cell (RBC) depleted whole blood. Blood was collected from healthy adult donors through venipuncture under sterile conditions with informed consent and approval of the Institutional Review Board of the University of California at Davis (protocol number 200311635-6). RBCs were removed using ammonia chloride based erythrocyte lysis solution (89.9 g of NH_4Cl, 10.0 g of $KHCO_3$, and 370.0 mg of tetrasodium EDTA in 10 L of deionized water) as described previously.[22] Leukocyte suspension was introduced into the flow chamber at a flow rate of 20 μL/min corresponding to a shear stress of ∼0.8 dyn/cm^2. Shear stress was calculated from the flow rate assuming an infinitely wide parallel-plate flow chamber.[43] The flow was stopped for 15 min to achieve T Cells capture after the chamber was filled

up with leukocyte suspension. In order to wash away nonspecifically bound cells, the flow rate was raised to 100 μL/min. Removal of the nonspecifically bound cells was typically complete after ~15 min.

Electrochemical Detection of IFN-γ. Electrochemical measurements were carried out using a CHI 842B potentiostat (CH Instruments, Austin, TX) operating inside a homemade Faraday cage. The electrochemical cell consisted of a flow-through Ag/AgCl (3 M KCl) reference electrode inserted at the outlet, a Pt wire counter electrode placed in the inlet of the microfluidic device, and Au working electrodes positioned inside the fluidic channels. Measurements were performed using SWV with a 40 mV amplitude signal at a frequency of −60 Hz over the range from −0.10 to −0.50 V. A homemade switching system was used to sample individual electrodes at predefined time intervals.

Calibration of the aptasensor was performed by infusing into a microchip known concentrations of IFN-γ (1−500 ng/mL) dissolved in RPMI1640 media buffer supplemented with 10% FBS. During detection of recombinant IFN-γ, a microchip was placed onto custom-made heating stage to maintain a temperature of 37 °C and to mimic conditions used in cell detection experiments (described below).

To analyze IFN-γ release from cells, microfluidic devices were incubated with RBC-depleted blood as described above. After T cells were captured, microfluidic devices were flushed with 1 × PBS and filled with mitogenic agents to commence cell activation and cytokine production. The mitogenic solution consisted of PMA and ionomycin dissolved to concentrations of 50 ng mL^{-1} and 2 mM, respectively, in phenol red-free RPMI1640 media supplemented with 10% FBS. A surgical clamp was secured around the inlet/outlet tubing to eliminate convective mixing. The microdevice was then placed on top of a heating stage (37 °C), and aptasensor electrodes were connected to a potentiostat via a multiplexer. As shown in Figure 1B, microchips contained 8 individually addressable electrodes, 4 electrodes per fluidic channel. One channel was used to measure IFN-γ release from mitogenically stimulated cells, whereas the other channel/set of electrodes was used to monitor cytokine production in unactivated leukocytes. In these experiments, SWV measurements were made every 15 min for up to 4 h.

Determination of IFN-γ Production Rates. Per cell IFN-γ production rates were calculated using COMSOL Multiphysics (COMSOL, Inc., Burlington, MA). A three-dimensional model was constructed based on a 3 × 10 × 0.1 mm microfluidic chamber. The average profile of measured IFN-γ concentrations at each electrode were then fit against the predicted values from the numerical simulation. Data from the first 60 min of production was fit, and a scaled least-squares regression was used to determine the best-fit production rate to 0.0001 pg/cell/h precision. Complete details are available in the Supporting Information.

RESULTS AND DISCUSSION

This paper details development of atpasensor arrays for detection of IFN-γ release from human T cells. The arrays of aptamer-modified electrodes were packaged in a nonfouling hydrogel and integrated with microfluidics to enable capture of CD4 T cells from a complex sample and continuous monitoring of IFN-γ release from these cells.

Surface Fabrication. The physical layout of the aptasensors is designed to aid in capturing the desired leukocyte subset in the immediate proximity of the aptamer-modified electrodes in order to enable detection of local concentration and maximize sensitivity (Figure 1A). Typical surface fabrication begins by microfabrication of Au electrodes onto glass slides. These slides are then modified with (3-acryloxypropyl)trichlorosilane in order to promote attachment of PEG hydrogel microstructures to glass regions. These acryloxy-functionalized regions serve a dual purpose: they promote hydrogel adhesion and support physisorption of proteins.[14] We take advantage of this surface functionality to precisely control cell attachment in proximity to our electrochemical sensors by patterning PEG hydrogel in an area around each electrode, leaving a small, well-defined ring-shaped area for adsorption of cell-capture antibodies. PEG hydrogel patterns are generated in this geometry by selective polymerization of a prepolymer solution exposed to UV light through a photomask aligned with the electrode geometry. Resultant micropatterned surfaces consisted of (1) circular Au electrodes (300 μm diameter), (2) ring-shaped glass regions adjacent to Au, and (3) nonfouling PEG hydrogel surrounding the Au/glass domains. A typical sensing unit comprised of a circular electrode (appearing black due to transmitted light microscopy), ring attachment area, and the surrounding PEG gel is shown in Figure 2A.

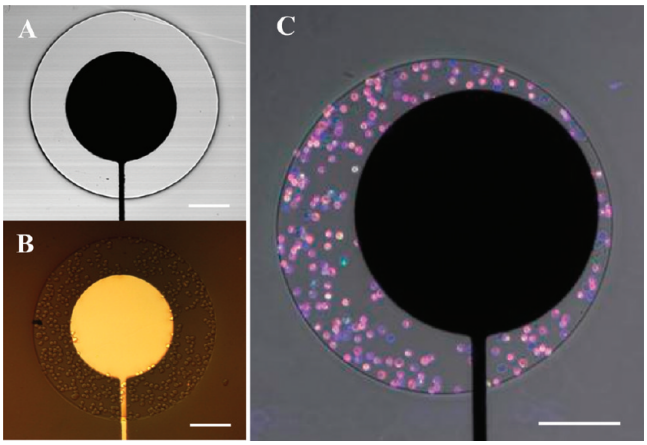

Figure 2. Micropatterned surfaces for capturing leukocytes next to sensing electrodes. (A) Au electrode inside a PEG hydrogel well prior to cell seeding. The ring-shaped glass region around the electrode contains anti-CD4 Abs. (B) Upright microscopy image showing cell attachment adjacent to but not on top of aptamer-modified electrodes. (C) Immunofluorescent staining with anti-CD3-FITC and anti-CD4-PE reveal that the majority of captured cells stain positive for both markers, pointing to the specific capture of CD4 T cells. T cells are also stained with DAPI (blue) to reveal the morphology of the nucleus. Please note the lack of nonspecific cell attachment on PEG gel regions of the micropatterned surface. Scale bars in each panel are 100 μm.

Spatially-Directed Cell Capture. After fabrication, electrode arrays are modified to deposit aptamer hairpin molecules to the electrode surfaces and the glass regions are modified with Abs for cell capture. In order to maximize sensitivity, we employ the above-described sensing surfaces to capture T cells in proximity to the functionalized electrodes. Selective adsorption of anti-CD4 Abs on glass attachment sites is shown in Figure S2, Supporting Information. The results from typical cell capture experiments are shown in Figure 2B and 2C. Upright microscopy imaging of the micropatterned surfaces show cells captured in the ring-shaped regions but not on PEG hydrogel regions or Au electrodes (Figure 2B). This underscores our ability to isolate cells in specific locations adjacent to sensing electrodes.

dx.doi.org/10.1021/ac202117g |*Anal. Chem.* XXXX, XXX, 000–000

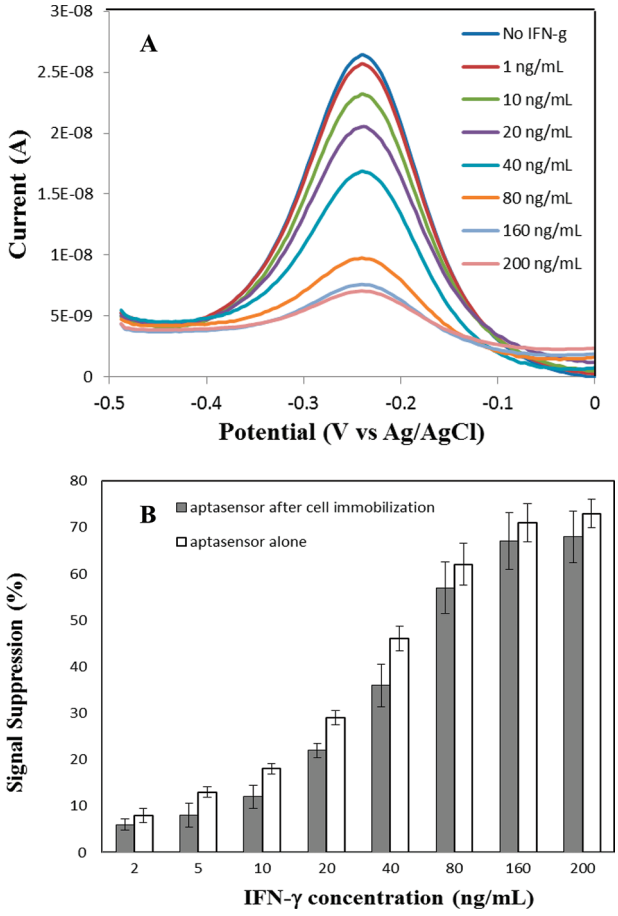

Figure 3. (A) Voltammograms obtained with SWV show a decrease in the faradaic current proportional to the solution concentration of recombinant IFN-γ. These results were obtained with gold electrodes modified with 0.5 μM concentration of aptamer. (B) Signal suppression plotted against recombinant IFN-γ concentration with and without Molt-3 cells captured in the device. As seen from these data, capture of cells did not impact aptasensor performance.

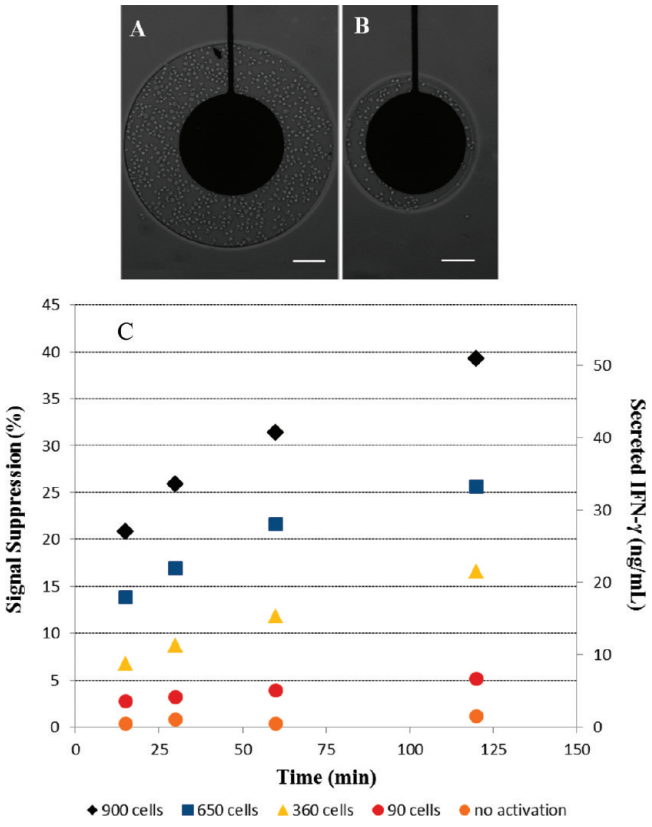

Figure 4. Continuous monitoring of IFN-γ release using aptamer-modified electrodes. (A and B) Capture of varying numbers of T cells in the glass attachment sites adjacent to sensing electrodes. These images show attachment of ~650 (A) and ~90 T cells (B); other electrodes in the same array contained 900 and 360 cells. (C) Aptasensor responses from different cell populations show that IFN-γ signal varied as a function of cell number with higher signal observed from larger cell populations. The calibration curve was used to convert signal suppression into IFN-γ concentration (right y axis). Scale bars are 100 μm.

Importantly, immunofluorescent staining reveals that captured cells are positive for CD3 and CD4 surface markers which defines the cells as $CD4^+$ T cells (Figure 2C and Figure S3, Supporting Information). Fluorescence images were used to determine the phenotype and purity of cells residing in the microwells. Immunofluorescent labeling with anti-CD3-FITC and anti-CD4-PE was used to identify CD3+ and CD4+ T cells. DAPI staining was used to determine the nuclear morphology of cells and evaluate nonspecific binding in the microwells. In order to determine the purity of captured cells, we enumerated the total number of CD3+ and CD4+ stained T cells and divided it by the total number of cells in the field of view. The purity of captured CD4 T cells was typically >90%.

Characterization of Aptasensor for IFN-γ Detection. We previously reported the development of an electrochemical aptasensor for IFN-γ detection.[37] This biosensor was based on aptamer hairpin with a MB redox label attached at the 5′-end and a thiol group at the 3′-end. Hairpin molecules were chemisorbed onto Au electrodes and exhibited a concentration-dependent change in electrical properties in the presence of IFN-γ, providing a signal used to detect IFN-γ. The change in electrical properties is attributed to unfolding of the hairpin and displacement of the redox moiety further from the electrode (see Figure 1A for schematic). SWV curves demonstrating the responses of aptasensors in the presence of varying concentrations of IFN-γ are shown in Figure 3A. Signal decreases as a function of increasing analyte concentration. This decrease in signal is often reported as "signal suppression": the ratio of SWV peak current loss at a given IFN-γ concentration to SWV peak current in the absence of analyte.

It is important to ensure that aptasensors remain functional after Ab immobilization and cell-capture steps. Therefore, experiments were undertaken to determine whether modification steps culminating with cell capture affected aptasensor performance. Aptasensor responses to exogenous IFN-γ were compared with and without cells present in the system (Figure 3B). Though a slight reduction in signal is observed, cell capture does not significantly impact aptasensor function or responsiveness. In the case when cells were seeded on the surface and when cells were absent, sensing electrodes for both scenarios exhibit similar detection limits near 60 pM and show linear responses over the expected range (from 60 pM to 9 nM). The limit of detection was derived using three times the standard deviation of the signal from at least three consecutive SWV scans in the absence of exogenous IFN-γ.

dx.doi.org/10.1021/ac202117g |*Anal. Chem.* XXXX, XXX, 000–000

In addition to sensitivity, it is also necessary that a sensor responds exclusively to the targeted molecule of interest. This is particularly important in IFN-γ detection since activated leukocytes are expected to secrete a number of additional cytokines (e.g., TNF-α and IL-2). The specificity of IFN-γ aptasensor was confirmed by challenging aptasensors to a high concentration of nonspecific cytokines (e.g., IL-2, TNF-α) known to be secreted by activated T cells on the time scale of hours[24] (see Figure S4, Supporting Information).

Continuous Monitoring of IFN-γ Release from CD4 T Cells. To show the utility of our aptasensor we demonstrate the real-time detection of local IFN-γ release from small groups of CD4 T cells. In a typical experiment, T cells were captured next to aptasensing electrodes and then mitogenically activated to commence cytokine production. Cells were captured but not activated in an independent microfluidic chamber on the same chip, providing a negative control. In order to verify measurement of local concentration, electrodes with an array were embedded in a PEG gel layer so as to define ring-shaped cell attachment sites of varying dimensions (50, 100, 150, or 200 μm). In an experiment described in Figure 4 these increasingly result in the capture of 90, 360, 650, and 900 cells adjacent to individual electrodes. Figure 4A and 4B shows micropatterned surfaces with 650 and 90 captured cells. Upon activation, IFN-γ release was simultaneously monitored at each member of the electrode array by performing SWV measurements every 15 min for up to 4 h. Results from a typical experiment are shown in Figure 4C. For the sake of simplicity, data for only one group of unactivated T cells are shown.

Electrochemical detection results in Figure 4C reveal that responses of electrodes within the same array vary as a function of cell number, with higher IFN-γ signals correlating to larger cell populations. The IFN-γ signal can be monitored over time, with detectable signal appearing as early as 15 min poststimulation from as few as 90 cells. Modeling diffusion using numerical approaches (COMSOL) reveals that cytokine gradients extend to ~1.5 mm from the cells, underscoring the importance of measuring local concentrations. Importantly, based on the experimental design, the total amount of released IFN-γ is highly dependent on the number of immobilized cells near the electrodes. This number (the number of immobilized cells) for each microwell varies from experiment to experiment. In order to address the reproducibility of this detection method, three independent experiments were carried out using the same blood sample. After normalizing the concentration of secreted IFN-γ with captured cell number, standard deviation from each time point was obtained from monitoring the same blood sample in three different experiments. Results are shown in Figure S7, Supporting Information.

Another parameter to consider is sensor response time. Starting from infusion of RBC-lysed blood into the microfluidic devices a total of ~15 min is needed to detect secretion of IFN-γ from as few as 90 cells. Besides introduction of cells only one additional step was needed to inject mitogens to commence cytokine production. This makes our approach a lot faster and simpler than the standard Ab-based immunological methods that typically utilize 100 000−1 000 000 cells, call for 6−12 h of activation, and take an additional 2−4 h to complete due to multiple washing and staining steps involved.

Diffusion modeling results also suggest that in the present configuration of the array an electrode begins sensing significant amounts of cytokines (>10% of detected analyte) produced at the neighboring electrode after ~4 h of stimulation. Signals detected at shorter times should be attributed to cells captured right next to the sensing electrode.

Determination of IFN-γ Production Rates. In addition to affording rapid detection, dynamic measurements of local IFN-γ concentration also allow us to estimate the rate of IFN-γ production in the system by considering the transport of the analyte within the microfluidic device. Because the measurements are conducted inside microchambers and the fluid is unstirred, transport of IFN-γ from the cells to the sensing electrode is purely diffusion mediated. Taking into consideration the positions of the captured cells and the electrodes, we are able to model this diffusion using a numerical approach (COMSOL Multiphysics). Our model reproduces the observed average time-dependent concentration profiles (Figure S5, Supporting Information) with excellent fidelity. Time-dependent concentration data from 3 experiments were averaged together to account for sample-to-sample variations in electrode positioning and cell behavior. The average IFN-γ production rate measured in our microdevices is estimated to be 0.0079 pg cell^{-1} h^{-1}, whereas rates reported by other groups using ELISA methods varied from 0. 00013 to 0.0043 pg cell^{-1} h^{-1}.[44−46] The slight discrepancy in results may be attributed to differences in how measurements are done. Our experiments reveal that the rate of IFN-γ production is not constant and decreases as a function of time. We are reporting a higher production rate occurring at early time points ($t \leq 1$ h), whereas the standard ELISA approaches average production over 12−24 h. This may explain the higher rate of IFN-γ production reported in the present study.

Verification of Sensor Performance in Cellular Environment. While aptamers are generally considered to be chemically stable, they are susceptible to digestion with nucleases.[47−49] In order to eliminate the possibility that nucleases released from cells contribute to the sensor response we examined the performance of aptasensors after use with activated leukocytes. Aptasensors were employed for detection of cytokine release from mitogenically activated cells as described above. Subsequently, cells were removed and aptasensors were regenerated by brief exposure to 7 M urea buffer. These "used" aptasensors (aptasensors have been used for detecting IFN-γ from live leukocytes) were then challenged with varying concentrations of recombinant IFN-γ and compared to pristine aptasensors that did not interact with cells and therefore could not have been exposed to endogenous nucleases. We observe no significant difference between IFN-γ responses of pristine vs used biosensors (see Figure S6, Supporting Information), suggesting that endogenous nucleases do not interfere with sensor responses. Our results also point to the possibility of reusing sensing devices.

CONCLUSIONS

Development of biosensors capable of rapid and simple detection of cell-secreted cytokines has significant implications in blood diagnostics. Herein, we describe a novel microdevice employing microfluidics, aptasensors, and surface micropatterning to capture CD4 T cells from a heterogeneous cell sample and to detect local IFN-γ release in real time. Micropatterning of sensing surfaces is used to ensure capture of the desired cell type and cell number in the immediate vicinity of aptamer-modified sensing electrodes. Sensitivity of the aptasensor and close proximity of cells to sensing electrodes allows detection of IFN-γ production from as few as 90 T cells after 15 min of mitogenic activation. Furthermore, use of aptasensing electrode arrays

enables simultaneous monitoring of cytokine production from several groups of cells. Given the importance of detecting leukocyte-secreted IFN-γ in a number of infectious diseases including TB and HIV, the availability of a microdevice for rapid, simple, and robust measurements of this cytokine has significant implications in immunology research and diagnostics. In addition, the dynamic cytokine production data recorded by this aptasensor may, in the future, provide a new basis for leukocyte phenotyping and disease diagnosis. Work is currently underway to develop aptasensors simultaneous detection of multiple cytokines and for single cell analysis.

■ ASSOCIATED CONTENT

Supporting Information. Protection of electrode arrays during Ab deposition; localization of Abs on micropatterned sensing surfaces; immunofluorescent staining of captured leukocytes; specificity of aptasensor electrodes; transport considerations and determination of IFN-γ production rates; stability of aptasensors; reproducibility of aptasensors. This material is available free of charge via the Internet at http://pubs.acs.org.

■ AUTHOR INFORMATION

Corresponding Author

*Phone: 530-752-2383. E-mail: arevzin@ucdavis.edu.

■ ACKNOWLEDGMENT

Financial support for this project was provided by the National Science Foundation (EFRI grant no. 0937997) and by the National Institutes of Health (Davis-Lawrence Livermore National Laboratories Point-of-Care Technologies Center pilot grant EB007959).

■ REFERENCES

(1) Douek, D. C.; Brenchley, J. M.; Betts, M. R.; Ambrozak, D. R.; Hill, B. J.; Okamoto, Y.; Casazza, J. P.; Kuruppu, J.; Kunstman, K.; Wolinsky, S.; Grossman, Z.; Dybul, M.; Oxenius, A.; Price, D. A.; Connors, M.; Koup, R. A. *Nature* **2002**, *417*, 95–98.

(2) Pantaleo, G.; Harari, A. *Nat. Rev. Immun.* **2006**, *6*, 417–423.

(3) Reece, W. H. H.; Pinder, M.; Gothard, P. K.; Milligan, P.; Bojang, K.; Doherty, T.; Plebanski, M.; Akinwunmi, P.; Everaere, S.; Watkins, K. R.; Voss, G.; Tornieporth, N.; Alloueche, A.; Greenwood, B. M.; Kester, K. E.; McAdam, K.; Cohen, J.; Hill, A. V. S. *Nat. Med.* **2004**, *10*, 406–410.

(4) Romagnani, S. *Clin. Immunol. Immnopathol.* **1996**, *80*, 225–235.

(5) Clerici, M.; Hakim, F. T.; Venzon, D. J.; Blatt, S.; Hendrix, C. W.; Wynn, T. A.; Shearer, G. M. *J. Clin. Invest.* **1993**, *91*, 759–765.

(6) Boehm, U.; Klamp, T.; Groot, M.; Howard, J. C. *Annu. Rev. Immunol.* **1997**, *15*, 749–795.

(7) Flynn, J. L.; Chan, J.; Triebold, K. J.; Dalton, D. K.; Stewart, T. A.; Bloom, B. R. *J. Exp. Med.* **1993**, *178*, 2249–2254.

(8) Harari, A.; Vallelian, F.; Pantaleo, G. *Eur. J. Immunol.* **2004**, *34*, 3525–3533.

(9) Maino, V. C.; Picker, L. J. *Cytometry* **1998**, *34*, 207–215.

(10) Cox, J. H.; Ferrari, G.; Janetzki, S. *Methods* **2006**, *38*, 274–282.

(11) Leng, S. X.; McElhaney, J. E.; Walston, J. D.; Xie, D. X.; Fedarko, N. S.; Kuchel, G. A. *J. Gerontol. A: Biol.* **2008**, *63*, 879–884.

(12) Toner, M.; Irimia, D. *Annu. Rev. Biomed. Eng.* **2005**, *7*, 77–103.

(13) El-Ali, J.; Sorger, P. K.; Jensen, K. F. *Nature* **2006**, *442*, 403–411.

(14) Revzin, A.; Sekine, K.; Sin, A.; Tompkins, R. G.; Toner, M. *Lab Chip* **2005**, *5*, 30–37.

(15) Chen, D. S.; Soen, Y.; Stuge, T. B.; Lee, P. P.; Weber, J. S.; Brown, P. O.; Davis, M. M. *PloS Med.* **2005**, *2*, 1018–1030.

(16) Soen, Y.; Chen, D. S.; Kraft, D. L.; Davis, M. M.; Brown, P. O. *PloS Biol.* **2003**, *1*, 429–438.

(17) Bailey, R. C.; Kwong, G. A.; Radu, C. G.; Witte, O. N.; Heath, J. R. *J. Am. Chem. Soc.* **2007**, *129*, 1959–1967.

(18) Kim, H.; Cohen, R. E.; Hammond, P. T.; Irvine, D. J. *Adv. Mater.* **2006**, *16*, 1313–1323.

(19) Bradshaw, E. M.; Kent, S. C.; Tripuraneni, V.; Orban, T.; Ploegh, H. L.; Hafler, D. A.; Love, J. C. *Clin. Immunol.* **2008**, *129*, 10–18.

(20) Love, J. C.; Ronan, J. L.; Grotenbreg, G. M.; van der Veen, A. G.; Ploegh, H. L. *Nat. Biotechnol.* **2006**, *24*, 703–707.

(21) Han, Q.; Bradshaw, E. M.; Nilsson, B.; Hafler, D. A.; Love, J. C. *Lab Chip* **2010**, *10*, 1391–1400.

(22) Zhu, H.; Stybayeva, G. S.; Macal, M.; George, M. D.; Dandekar, S.; Revzin, A. *Lab Chip* **2008**, *8*, 2197–2205.

(23) Zhu, H.; Stybayeva, G. S.; Silangcruz, J.; Yan, J.; Ramanculov, E.; Dandekar, S.; George, M. D.; Revzin, A. *Anal. Chem.* **2009**, *81*, 8150–8156.

(24) Stybayeva, G.; Mudanyali, O.; Seo, S.; Silangcruz, J.; Macal, M.; Ramanculov, E.; Dandekar, S.; Erlinger, A.; Ozcan, A.; Revzin, A. *Anal. Chem.* **2010**, *82*, 3736–3744.

(25) Stybayeva, G.; Kairova, M.; Ramanculov, E.; Simonian, A. L.; Revzin, A. *Colloid Surf. B* **2010**, *80*, 251–255.

(26) Boom, H. *Infect. Agents Dis.* **1996**, *5*, 73–81.

(27) Urata, H.; Nomura, K.; Wada, S.; Akagi, M. *Biochem. Biophys. Res. Commun.* **2007**, *360*, 459–463.

(28) Tang, Z. W.; Mallikaratchy, P.; Yang, R. H.; Kim, Y. M.; Zhu, Z.; Wang, H.; Tan, W. H. *J. Am. Chem. Soc.* **2008**, *130*, 11268.

(29) Li, W.; Yang, X. H.; Wang, K. M.; Tan, W. H.; Li, H. M.; Ma, C. B. *Talanta* **2008**, *75*, 770–774.

(30) Xiao, Y.; Piorek, B. D.; Plaxco, K. W.; Heeger, A. J. *J. Am. Chem. Soc.* **2005**, *127*, 17990–17991.

(31) Radi, A. E.; Sanchez, J. L. A.; Baldrich, E.; O'Sullivan, C. K. *J. Am. Chem. Soc.* **2006**, *128*, 117–124.

(32) Lu, Y.; Li, X. C.; Zhang, L. M.; Yu, P.; Su, L.; Mao, L. Q. *Anal. Chem.* **2008**, *80*, 1883–1890.

(33) Xiao, Y.; Lubin, A. A.; Heeger, A. J.; Plaxco, K. W. *Angew. Chem., Int. Ed.* **2005**, *44*, 5456–5459.

(34) Bock, C.; Coleman, M.; Collins, B.; Davis, J.; Foulds, G.; Gold, L.; Greef, C.; Heil, J.; Heilig, J. S.; Hicke, B.; Hurst, M. N.; Husar, G. M.; Miller, D.; Ostroff, R.; Petach, H.; Schneider, D.; Vant-Hull, B.; Waugh, S.; Weiss, A.; Wilcox, S. K.; Zichi, D. *Proteomics* **2004**, *4*, 609–618.

(35) Shangguan, D.; Li, Y.; Tang, Z. W.; Cao, Z. H. C.; Chen, H. W.; Mallikaratchy, P.; Sefah, K.; Yang, C. Y. J.; Tan, W. H. *Proc. Natl. Acad. Sci. U.S.A.* **2006**, *103*, 11838–11843.

(36) Liu, J. W.; Mazumdar, D.; Lu, Y. *Angew. Chem., Int. Ed.* **2006**, *45*, 7955–7959.

(37) Liu, Y.; Tuleouva, N.; Ramanculov, E.; Revzin, A. *Anal. Chem.* **2010**, *82*, 8131–8136.

(38) Zhu, H.; Yan, J.; Revzin, A. *Colloid Surf. B* **2008**, *64*, 260–268.

(39) Revzin, A.; Tompkins, R. G.; Toner, M. *Langmuir* **2003**, *19*, 9855–9862.

(40) Xiao, Y.; Lai, R. Y.; Plaxco, K. W. *Nat. Protoc.* **2007**, *2*, 2875–2880.

(41) Whitesides, G. M.; Ostuni, E.; Takayama, S.; Jiang, X.; Ingber, D. E. *Annu. Rev. Biomed. Eng* **2001**, *3*, 335–373.

(42) Schaff, U. Y.; Xing, M. M. Q.; Lin, K. K.; Pan, N.; Jeon, N. L.; Simon, S. I. *Lab Chip* **2007**, *7*, 448–456.

(43) Sekine, K.; Revzin, A.; Tompkins, R. G.; Toner, M. *J. Immunol. Methods* **2006**, *313*, 96–109.

(44) Bailer, R. T.; Holloway, A.; Sun, J. W.; Margolick, J. B.; Martin, M.; Kostman, J.; Montaner, L. J. *J. Immunol.* **1999**, *162*, 7534–7542.

(45) Munder, M.; Mallo, M.; Eichmann, K.; Modolell, M. *J. Exp. Med.* **1998**, *187*, 2103–2108.

(46) Slifka, M. K.; Whitton, J. L. *J. Immunol.* **2000**, *164*, 208–216.

(47) Avery, O. T.; MacLeod, C. M.; McCarty, M. *J. Exp. Med.* **1944**, *79*, 137–158.

(48) Linn, S.; Arber, W. *Proc. Natl. Acad. Sci. U.S.A.* **1968**, *59*, 1300.

(49) Arber, W.; Linn, S. *Annu. Rev. Biochem.* **1969**, 467–500.